Experimental Facilities and Modelling for Rarefied Aerodynamics

Elena Kustova, Andrey Krylov, Valeriy Lashkov, Mariya Mekhonoshina
Saint Petersburg State University
Department of Mathematics and Mechanics
28 Universitetskiy prospect
198504 Saint Petersburg, Russia

elena_kustova@mail.ru

ABSTRACT

The present lecture is devoted to experimental and theoretical modelling for rarefied aerodynamics. General features of experimental studies in rarefied flows are discussed. Experimental facilities designed in Saint Petersburg State University for rarefied aerodynamics and plasma flow control are described. Several theoretical models for non-equilibrium reacting flows in the slip regime are presented.

1.0   INTRODUCTION

"Aerodynamics of rarefied gases is a branch of mechanics of gases in which their molecular structure must be taken into account in describing their motion. The methods of rarefied aerodynamics are widely applied in the determination of aerodynamic heating during the landing of orbital craft and for low-flying earth satellites, for the calculation of the thermal conditions of instrument transducers of rockets that are exploring the upper layers of the atmosphere, and so on. The exact prediction of the trajectories of low-altitude planetary satellites that are testing the braking action of rarefied atmosphere is impossible without knowledge of the methods of the aerodynamics of rarefied gases. Using these methods, it is possible to determine the aerodynamic forces and moments that act on an object moving in the gas. The aerodynamics of rarefied gases also investigates the flow of gases in vacuum systems, ultrasonic oscillations in gases, and other problems of molecular physics." – The Great Soviet Encyclopedia, 3d Edition (1979).

Originally, theoretical models for rarefied gas flows were developed in the frame of the molecular kinetic theory. Thus the first self-consistent descriptions of a weakly non-equilibrium gas flow were given by the Hilbert and Chapman-Enskog [1] asymptotic methods and later by the Grad's moment method [2]. In 1950-60-ies, the interest to the aerodynamics of vehicles at high altitudes became crucial due to the space exploration programs. The prospects of application of molecular approach to the solution of problems of aerodynamics were well understood in the nascent rarefied gas-dynamic community. Theoretical studies carried out at that time are summarized in [3, 4, 5]. Various methods for the solution of the Boltzmann equation were developed, among them linearized and model equations, integral and variational methods, that of discrete velocities and others [5, 6]. The next step in the theoretical rarefied aerodynamics was modelling of strongly non-equilibrium flows with internal degrees of freedom and chemical reactions. Modifications of the Chapman-Enskog method taking into account these effects were proposed in [7-11] and successfully applied for the calculations of different flows. For non-linear problems, the Direct Simulation by the Monte Carlo method (DSMC) was elaborated [12, 13] and, in the present time, it becomes the most popular and efficient tool for the modelling of transition and free molecular flows.

Experimental modelling for rarefied flows was rapidly progressing together with theoretical studies. First low density (vacuum) wind tunnels were built in NASA AMES centre, California University, University of Toronto (early 1950-ies), and approximately in the same time in the main Russian scientific centres. The general ideas of experimental facilities and measurement techniques for rarefied gases were formulated in [3] and received further development in the next decades.

Great advances in theoretical, experimental and numerical modelling for rarefied flows were achieved

during the more than 50-years history of Rarefied Gas Dynamics symposia. The first symposium was organized in Nice in 1959 and the last (27th) one in Pacific Grove (California) in 2010. In the proceedings of the RGD Symposia, one can find the most up-to-date theoretical and experimental results on rarefied aerodynamics.

2.0 GENERAL CONSIDERATION OF RAREFIED FLOWS

At high altitudes, the mean free path length l of molecules between collisions may become comparable with the characteristic dimension L of an object moving in the atmosphere (or the region of flow under consideration). Therefore, the continuum-based methods of flow calculation are not applicable, and it is necessary to use the kinetic theory of gases. At high gas temperatures encountered, for example, at very high flight velocities, the flow is accompanied by non-equilibrium processes such as excitation of internal energy, dissociation, and ionization of molecules. These problems are also studied in the rarefied aerodynamics.

The classification of rarefied flows is based on the Knudsen number Kn=l/L. Thus we can distinguish rarefied flows of three types:

- Free molecular flows, Kn >> 1

- Transition flows, Kn ~ 1

- Slip flows, or another words, weakly rarefied flows, Kn << 1 (Kn ~ 0.001– 0.25)

The medium can be considered as continuum if the Knudsen number tends to zero.

2.1 Free molecular regime

In a free molecular flow of molecules reflected from an object, the free path length l is greater than the object's characteristic dimension L, and so the interaction of the reflected molecules with the incident molecules near the object is insignificant. This makes it possible to consider the incident and reflected flow of molecules independently, which essentially facilitates the description of their motion. The motion of any molecule can be considered as consisting of two components: (1) the molecules take part in the directed motion of the gas flow and their velocity is equal to the mean flow velocity, (2) the molecules simultaneously take part in chaotic thermal motion and move with different velocities whose values are described by the Maxwell distribution. The application of the kinetic theory of gases makes possible the calculation of both the pressure of the gas on the wall and the amount of heat the wall gains or loses in interactions with gas molecules. In order to do this, it is necessary to know the laws of reflection of molecules from the surface.

However, the exact mathematical description of the motion of a rarefied gas by means of the equations of kinetic theory is rather difficult. Therefore, approximate methods have been developed. For example, the real reflection of molecules from an object is replaced by the so-called specular-diffusion scheme, according to which part of the molecules are reflected from the object's surface as from a mirror, and others are scattered diffusely in conformity with Lambert's law (the cosine law).

The ratio of the number of diffusely scattered molecules to the total number of impinging particles determines the degree of diffusion of scattering, which is characterized by the number σ (at $\sigma = 0$, only mirror-like reflection occurs; at $\sigma = 1$, only diffuse reflection). In order to reduce the drag of a flying object, mirror-like reflection is advantageous. Small angles of incidence of the molecules to the surface are also desirable because they increase the probability of specular reflection.

Another important parameter is the so-called thermal accommodation coefficient α, which characterizes the change in the molecule's energy after its reflection. The values of α can vary from 0 to 1. If after

reflection the energy of the molecule has not changed and remains equal to the energy of the incident molecule, then $\alpha = 0$. If the average energy of the reflected molecule corresponds to the temperature of the wall, that means that the molecule has given up all its possible energy to the wall, and $\alpha = 1$. It is obvious that aerodynamic heating decreases with decreasing α.

The quantities σ and α are the most important characteristics of free molecular flows. In the general case, α and σ depend on flow velocity of the gas, the material and temperature of the wall and the smoothness of its surface, the presence of adsorbed gas molecules on the surface, and so on. However, the exact dependences of α and σ on the parameters determining them are still not known.

Experiments conducted over a wide velocity range with various gases and materials have yielded α values over a wide range, from 0.95 to 0.02. It has been established that a decrease in α occurs when the velocity of the gas molecules and the ratio of the molecular masses of the object and the gas are increased. Thus, for example, if a lead object is used instead of an aluminum one, the coefficient of accommodation is reduced by a factor of about 4, which results in a reduction in aerodynamic heating. The coefficient σ changes less, from 0.98 to 0.7.

The rarefaction of the medium leads to the rather unusual behaviour of the aerodynamic coefficients. Thus, the drag coefficient of a sphere in a rarefied flow depends on the ratio of the absolute temperature of the object T_w to the absolute temperature of the flow T as well as on α and σ, whereas in a continuous medium such dependencies are not observed. The coefficients that characterize heat exchange also differ qualitatively and quantitatively from the continuous coefficients.

The free-molecular flow description is given by the kinetic theory of gases. In particular, analytical solutions were obtained for simple flows [5, 6]. For more complex flows, DSMC method [12, 13] is suitable.

2.2   Transition regime

For Kn ~ 1, the role of intermolecular collisions is significant since the molecules reflected from the object surface distort the velocity distribution of the molecules of the incident stream. The theoretical solutions obtained for free molecular flow are not suitable here. In addition, it is still not possible to consider such a flow as the flow of a continuous medium. The transition regime is very difficult to analyze mathematically. The best ways to describe transition flows are DSMC and numerical solution of the Boltzmann equation. The moment method of Grad is also suitable for flows with Kn ~ 1.

2.3   Slip regime

If the dimension of an object L is dozens of times larger than l, then the shock waves and boundary layers at the surface of objects, which are characteristic of continuum gas dynamics, can develop in the flow. However, in contrast to the ordinary boundary layer, the temperature T_a of the gas adjacent to the wall is not equal to the temperature of the wall T_w, and the flow velocity at the surface of the object is not 0 (the flow slips). The temperature jump $(T_w - T_a)$ is proportional to l and depends on α. The slip velocity is also proportional to l and depends on σ. Experiments have demonstrated that with the increase in rarefaction of the gas there is a thickening of the shock wave. The width of the boundary layer also increases, but considerably more slowly. The shock wave can propagate over the whole region of compressed gas in the region of the forward stagnation point of the streamlined object and combine with the boundary layer. The density distribution in the region of the forward stagnation point becomes smooth, not uneven as in a continuum. In the calculation of slip flows, the flow is described by the equations of gas dynamics, but with boundary conditions that take the temperature jump and the slip velocity into account.

In the slip flow regime, non-equilibrium effects become of importance, when the characteristic times of some microscopic processes are comparable with the mean time of gas-dynamic parameters variation. For

instance, at various flow altitudes, internal energy relaxation, chemical reactions, ionization may proceed on the gas-dynamic time scale. Under strongly non-equilibrium conditions, a reliable flow description is provided by modifications of the Chapman-Enskog method [7-11].

3.0 EXPERIMENTAL FACILITIES FOR RAREFIED FLOWS

3.1 Overview

Rarefied-gas (vacuum) wind tunnel is a wind tunnel operating at low pressures. The working gas enters to the working chamber either from a gas storage tank or from the atmosphere through the pressure regulating valve, heater and nozzle. In the working section surrounded by a vacuum chamber, the model and supporting devices as well as measuring systems are placed. Sometimes, behind the working chamber, a cylindrical diffuser is situated. Gas evacuation from the vacuum wind tunnel down to the pressures of 1– 0.01 Pa is carried out using a vacuum system basically consisted of successively installed mechanical (forevacuum) pumps and oil (oil-diffusion) pumps. Great advantages can be achieved if cryogenic pumps are used since they consume less power and are more compact compared to mechanical and oil pumps and, at the same time, provide better capacity. Vacuum wind tunnels equipped with cryogenic pumps can operate in both steady-state regime with low mass flow rate and impulse regime with high flow rate and operating time 0.1-5 s. In modern cryogenic vacuum facilities rarefaction up to 10^{-6} Pa can be obtained.

The degree of rarefaction is specified by the Knudsen number. Usual vacuum wind tunnels operate in the transition flow regimes ($0.25 < Kn < 10$) and slip regimes ($10^{-3} < Kn < 0.25$). When a converging-diverging (de Laval) nozzle is used for the creation of a rarefied flow, a boundary layer appears in the diverging part of a nozzle. Its thickness increases rapidly reducing the isentropic flow core and thus preventing the realization of a required regime. This problem can be avoided by using so-called under-expanded nozzles or diaphragms. Noticeable reduction of the boundary layer thickness can be achieved using boundary layer suction through porous nozzle walls or by wall cooling with liquid nitrogen. Vacuum wind tunnels operating in the transition and slip regimes are used for measurements of aerodynamic characteristics of vehicles at high altitudes such as forces and moments as well as thermal loads on the surface.

In order to obtain gas flows with $Kn > 10$, vacuum facilities equipped with a free-molecular beam are used. In their working chamber a separator and a set of perforated collimators are installed. From the gas flow accelerated in the nozzle, a free-molecular beam with the velocities equal in the direction and absolute value is extracted. The main part of the gas exiting the nozzle is evacuated by one set of pumps down to the pressure ~ $1–10^{-2}$ Pa, whereas the free-molecular beam is pumped down to the pressures of $10^{-2}–10^{-4}$ Pa using another set of pumps. This kind of vacuum wind tunnels is used for studies of gas-surface interaction, determination of scattering functions and accommodation coefficients.

For pressure measurements in vacuum lines and working section, various types of vacuum gages are used, mostly thermocouple- and ionization-based ones. Aerodynamic forces and moments are measured using an aerodynamic balance with resolution of a fraction of a milligram. Flow visualization is performed using glow discharges and electron beams.

3.2 Vacuum facility VU-1 of Saint-Petersburg State University

Vacuum facility VU-1 (see Figs. 1, 2) was built in the Gas-Dynamic Laboratory of Saint-Petersburg State university in the early 1960-th, when the scientific school of Professor Sergei Vallander was fast progressing, and the rarefied aerodynamics in the Soviet Union was of crucial importance due to the space exploration programs.
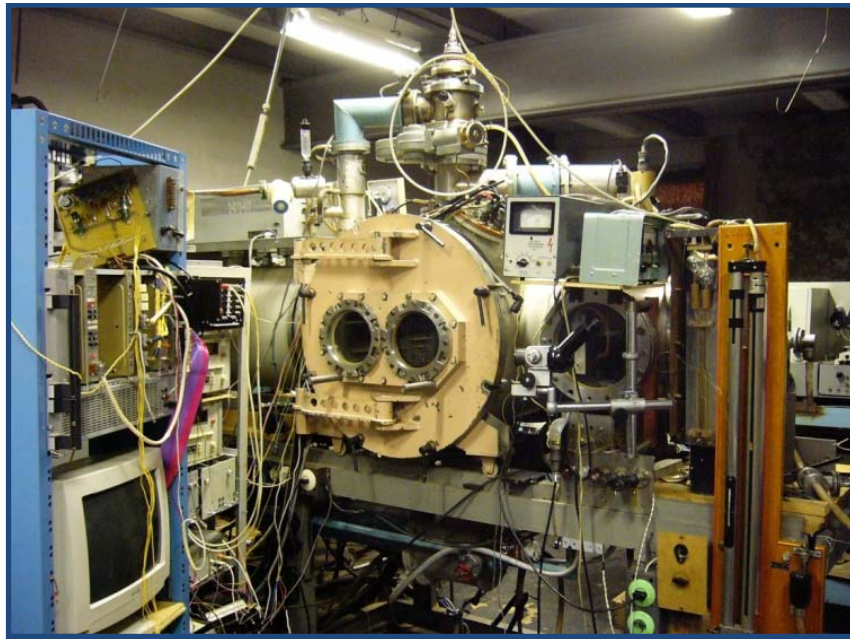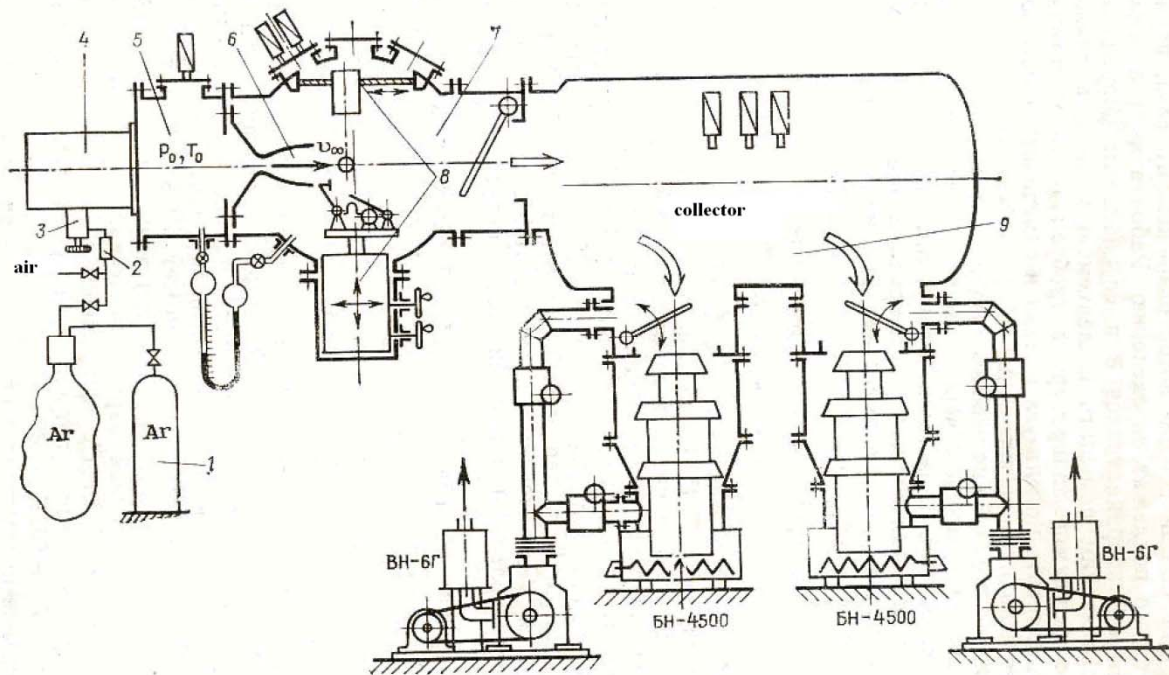
Figure 1: Vacuum facility VU-1

Figure 2: Schematic diagram of the vacuum facility VU-1.
1 – gas storage tank; 2 – drier; 3 – leak valve; 4 – heater; 5 - settling chamber; 6 – nozzle;
7 – working section; 8 – coordinate system; 9 – gas evacuation system

The schematic diagram of the wind tunnel is given in Fig. 2. The system of preliminary gas preparation consists of the gas storage tank 1, drier 2, and special leak valve 3 which provides the required flow rate from the storage tank. The system of the rarefied flow formation includes gas heater 4, settling chamber 5, and nozzle 6. While passing through the heater, the gas is heated up to the temperature necessary to

prevent condensation. In the settling chamber, all the flow parameters are equalized, and the gas flow becomes equilibrium. The cross section of the chamber is large enough to neglect the flow velocity and assume that the gas is in the rest. In the settling chamber, stagnation parameters p_0 and T_0 are measured. In order to create the rarefied flow, a supersonic conic or shaped nozzle is used.

Experiments are conducted in the working section 7. It is equipped with the coordinate system and special devices making it possible to place the model and gages into the required flow point, to set the angle of attack, and to measure aerodynamic forces.

Gas evacuation system is designed for the gas removal from the test section and pressure maintenance. It includes various vacuum pumps, vacuum collector, and vacuum shutters. The evacuation system operates in two test section pressure regimes:

(1) $p = 10^{-2} – 5 \cdot 10^{-3}$ Torr

(2) $p > 1$ Torr

The first regime is provided by two boost diffusion pumps and mechanical vacuum pumps. To maintain the second regime, two mechanical vacuum pumps are sufficient. The capacity of the evacuation system is one of the most important characteristics of the wind tunnel specifying the flow rate through the nozzle and, therefore, the size of the isentropic flow core at a given velocity. The capacity of the wind tunnel VU-1 is 0.1 g/s at the pressure 10^{-2} Torr. The main characteristics of the facility are given in Table 1.

Flight altitudes	100–30 km
Diameter of the working flow	up to 30mm
Mach number	0.8–7.0
Maximum Knudsen number	1.5
Reynolds numbers	$10–10^3$
Stagnation temperature	1300 K (ohmic heating) 2500 K (plasma heating)
Working gas	Air, N_2, CO_2, propane
Maximum factor of jet under-expansion	10^3
Maximum electrical power	65kW

Table 1: Characteristics of the vacuum facility VU-1

The facility is equipped with the three-component magneto-electrical aerodynamic balance for measurements of forces and moments. The forces are measured in the range 1 mg – 50 g. Measurements of local normal and tangential stresses on the body surface are carried out using the new original technique of floating element which allows measuring of stresses under non-equilibrium conditions. The accuracy of normal stress measurements is one order of magnitude higher than that obtained by traditional draining methods. While tangential stresses are measured, the registered surface forces in the base region can be of the order of 10^{-6} g. The facility has been recently upgraded with modern diagnostic tools including laser

and optical methods; spectral methods for studying relaxation processes, electron-beam methods allow registration of concentrations in gas-mixture flows.

Figure 3: Long-term orbital station and Buran models studied in VU-1
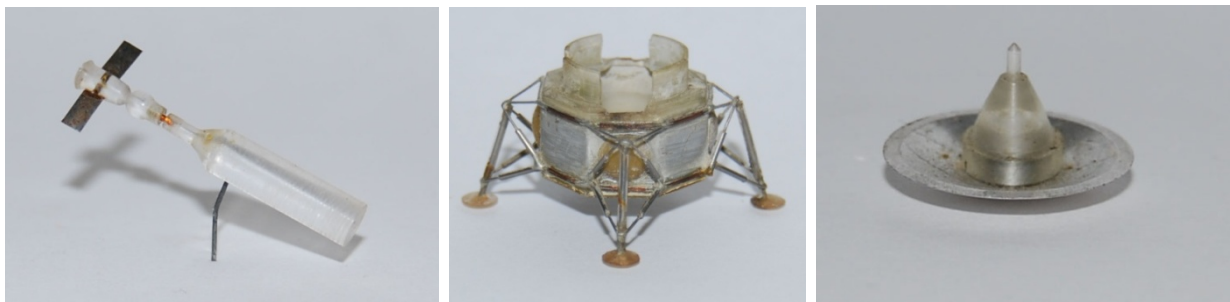

Figure 4: Docking model Soyuz-Apollo; Moon descent module; Mars descent module

In the VU-1 wind tunnel, studies for external aerodynamics were performed for both simple-geometry bodies and reentering vehicles of various shapes as well as for space vehicles and their modules (see Figs. 3-4). Practically all Russian space objects were tested in this facility under orbital and reentry regimes, experimental campaigns in the frame of Moon, Venus, and Soyuz-Apollo programs were carried out. The influence of different factors such as rarefaction degree, Mach number, angle of attack on the aerodynamic forces and moments was evaluated. One of the main objectives was to study the effects of mutual aerodynamic interference which is of crucial importance for emergency undocking. Interference effects can qualitatively modify aerodynamic characteristics of vehicles. Systematic studies for local convective heat exchange for bodies of simple and special shapes were also conducted.

Another part of the VU-1 facility is the gas-dynamic test stand. Using this stand, the structure of under-expanded jets and their interaction with obstacles differently oriented towards the flow were widely studied. In particular, aerodynamic moments of the Moon descent module were investigated taking into account the lunar terrain features, craters, and dusty flow reflected from the surface. The floating element technique was applied for normal and tangential stress measurements.

In the present time, the vacuum wind tunnel is used for the development of new gas-jet flow control techniques aimed to reduce aerodynamic forces and heat fluxes acting on a vehicle. The main idea is in ejecting, towards the main flow, an additional gas mass in the form of an under-expanded jet. As the result of flow-jet interaction, the local shock wave structure is created before the vehicle nose connected to the body via the jet. The momentum and the energy of the supersonic flow are dissipated before the vehicle

thus reducing the drug and the heat flux.

The vacuum facility VU-1 can be further upgraded and used for studying new problems of rarefied aerodynamics.

3.3   Supersonic wind tunnel TB-3

Wind tunnel TB-3 (Fig.5) is a supersonic wind tunnel, designed to study supersonic aircrafts, single and block jets and their interaction with obstacles, plasma – body interaction. Its main characteristics are given in Table 2.
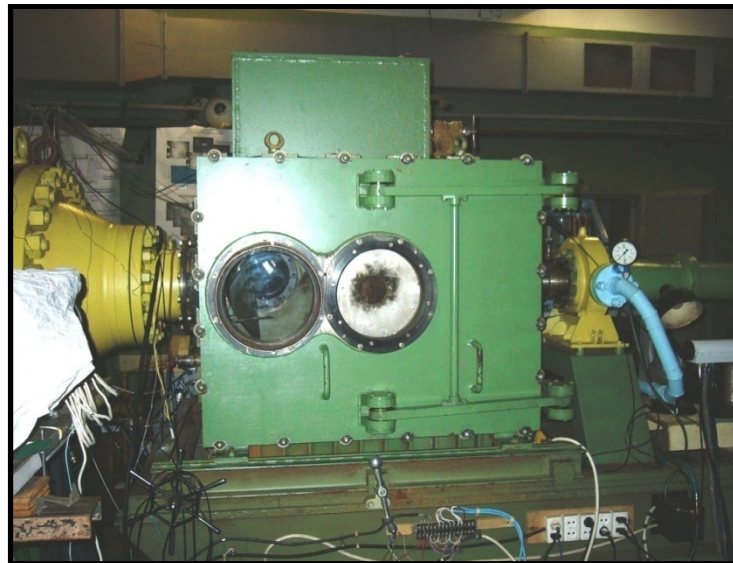

Figure 5: Supersonic wind tunnel TB-3

Diameter of the working flow	up to 60mm
Mach number	1.1-3
Static pressure	25-70 Torr
Stagnation pressure	Up to 200 atm
Stagnation temperature	600 K
Working gas	Air, N_2, CO_2
Ejector for creation rarefied working flows	

Table 2: Characteristics of the supersonic wind tunnel TB-3

At the present time, TB-3 is mainly used to investigate the interaction of a microwave discharge with gas dynamic structures. These operations are conducted in order to develop new ways of improving the aircrafts aerodynamic characteristics and reducing the heat flux at hypersonic speeds, in particular, to study the possibility of microwave energy deposition for flow/flight control. The wind tunnel is equipped with the powerful microwave generator providing pulse microwave power 210kW, duration 1.5mcs; it is

equipped also with modern diagnostic tools for optical, power, temperature measurements for non-stationary interaction of the microwave discharge with the shock layer in the vicinity of the model in a supersonic flow.
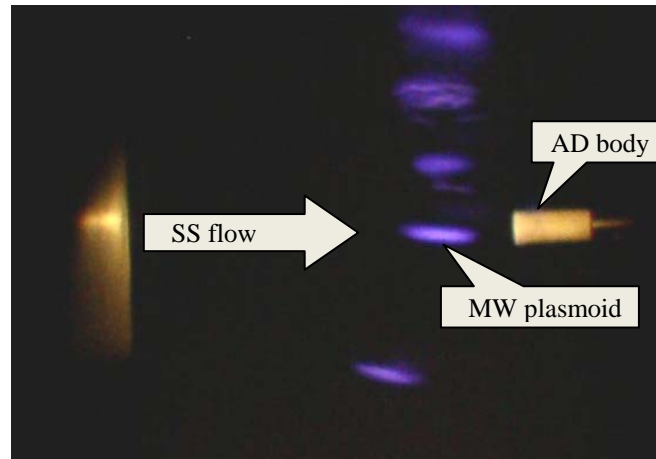

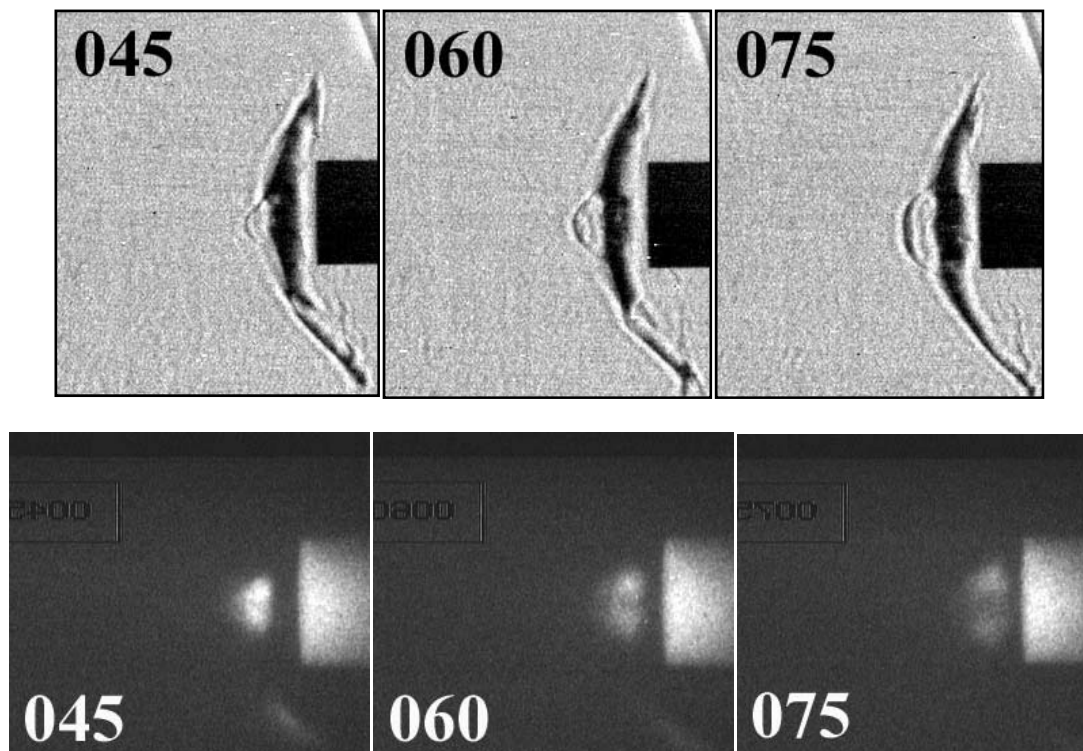**Figure 6: Scheme of experiment**

Figure 7: Different phases of the plasma to body interaction.

In Fig. 6, the principle scheme of experiment [14, 15] is presented. A microwave (MW) discharge is created near the blunt cylinder of 20 mm diameter with central axis coinciding with that of symmetry of the main MW plasmoid. In the present experiment, a supersonic flow with M=2.1 is studied. Different phases of the plasma to body interaction are registered using various optical devices. Typical results of flow visualization at different times are given in Fig. 7. Numbers on the images indicate the time interval (in microseconds) after MW discharge termination. While images in the upper row are registered using the

Schlieren technique, those in the lower row are obtained by means of a special visualizing system based on a CCD camera and three-cascade electronic-optical amplifier (EOA) with an electronic gate.

The nearest to the body tip of plasmoid at the moment of its creation is located within several millimeters upstream from the bow shock wave. The interaction starts after about 20 mcs, which can be clearly seen from the chemiluminescent image due to the intensification of light emission behind the shock (the emission intensity is proportional to the squared density). On the Schlieren image, one can see the blast wave originated from the plasmoid and propagating away from it. The next time period refers to preceding the complete absorption of plasmoid by the shock layer. By this moment, the emitting agent has already fulfilled the entire volume of the structure. Analyzing Fig. 7 one can observe also vortex formation and development inside the shock layer.
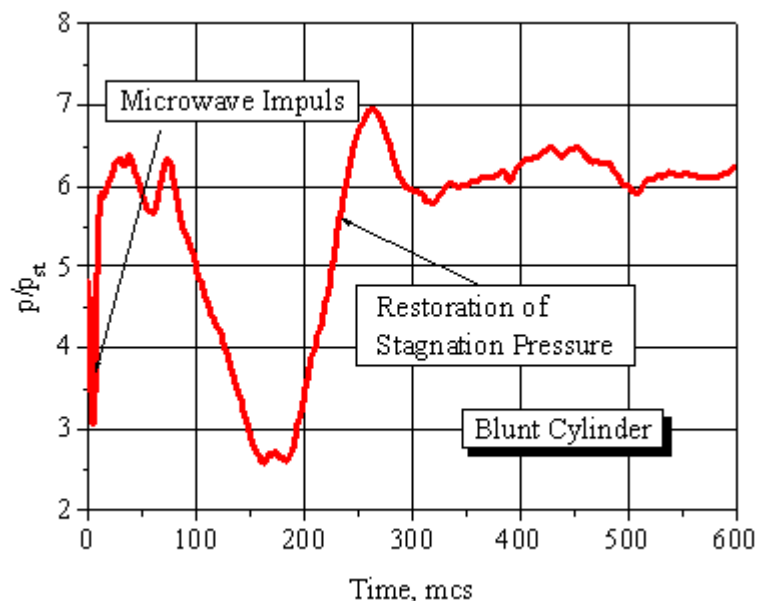

Figure 8: Different phases of the plasma to body interaction.

Several main stages of the process can be distinguished:

- the moment of MW discharge. After about 20 mcs, the discharge region touches the bow shock wave;

- discontinuity decay, the shock wave moves along the heated channel. The upstream velocity of shock movement (in the laboratory frame) is about 0.22-0.25mm/mcs, or 0.45-0.5 of the flow (bow shock) velocity;

- vortex creation and its extension (this process seems to start even earlier, at 35 mcs, but it is not well distinguished due to screening of the main part of the bow shock);

- decay of the vortex, vortex disintegration;

- reconstruction of primary streamlining. The process of the bow shock relaxation to the stationary state takes 100 mcs longer and represents gradual movement (with oscillations) to a nominal position.

The time-resolved signal from pressure sensor obtained in this experiment is shown in Fig. 8. It is seen that the intensive pressure fall down starts at about 70 mcs. This is the moment when the vortex already occupies the area in the shock layer just in the vicinity of the front surface and begins to interact with it. The process of interaction and gradual vortex blow-down lasts about 150 mcs. During this phase, the stagnation pressure drops down from 215 Torr (its nominal value) to about 70 Torr, or 3 times. This

lowest value is attained at about 160 mcs. The unperturbed value of the stagnation pressure is attained after about 300 mcs.

Thus we can see that an efficient energy deposition to the supersonic flow results in flow reorganization, modification of the shock wave structure in front of the body, and reducing the total energy required for the vehicle motion. This can be used for improving the aerodynamic characteristics of the vehicle.

4.0   THEORETICAL MODELLING FOR RAREFIED SLIP FLOWS

The main feature of rarefied flows in the slip regime is that molecular effects such as excitation of internal energy, chemical reactions, and ionization can affect the macroscopic gas flow parameters. Moreover, physical-chemical processes often proceed on the gas-dynamic time scale thus creating strongly non-equilibrium conditions in a flow.

The first attempt to take into account the excitation of internal degrees of freedom in calculations for the transport coefficients was made in 1913 by E. Eucken [16], who introduced a phenomenological correction into the formula for the thermal conductivity coefficient. Later on, stricter analysis for the influence of the excitation of internal degrees of freedom of molecules on heat and mass transfer was based on the kinetic theory of gases. Originally, in the papers concerning kinetic theory models for transport properties, mainly minor deviations from the local thermal equilibrium were considered for non-reacting gases [17] and for mixtures with chemical reactions [9]. In this approach non-equilibrium effects were taken into account in transport equations by introducing supplementary kinetic coefficients: the coefficient of volume viscosity in the expression for the pressure tensor and corrections to the thermal conductivity coefficient in the equation for the total energy flux. Such a description of the real gas effects becomes insufficient under the conditions of finite (not weak) deviations from the equilibrium, in which the energy exchange between some degrees of freedom and some part of chemical reactions proceed simultaneously with the variation of gas-dynamic parameters. In this case characteristic times for gas-dynamic and relaxation processes become comparable, and therefore the equations for macroscopic parameters of the flow should be coupled to the equations of physical-chemical kinetics. The transport coefficients, heat fluxes, diffusion velocities directly depend on non-equilibrium distributions, which may differ substantially from the Boltzmann thermal equilibrium distribution. In this situation, the estimate for the impact of non-equilibrium kinetics on gas-dynamic parameters of a flow and its dissipative properties becomes especially important. In recent years, these problems receive much attention, and new results have been obtained in this field on the basis of the generalized Chapman-Enskog method [7-11]. The kinetic theory makes it possible to develop mathematical models of a flow under different non-equilibrium conditions, i.e. to obtain closed systems of the non-equilibrium flow equations and to elaborate calculation procedures for transport and relaxation properties.

The theoretical models adequately describing physical-chemical kinetics and transport properties in a flow depend on relations between relaxation times of various kinetic processes. Experimental data show the significant difference in relaxation times of various processes.

At the high temperature conditions which are typical just behind the shock front, the equilibrium over the translational and rotational degrees of freedom is established for a substantially shorter time than that of vibrational relaxation and chemical reactions, and therefore the following relation takes place [18, 19]:

$$\tau_{el} \sim \tau_{rot} \ll \tau_{vibr} < \tau_{react} \sim \theta \tag{1}$$

Here, τ_{el}, τ_{rot}, τ_{vibr}, and τ_{react} are, respectively, the relaxation times for the translational, rotational and vibrational degrees of freedom, and the characteristic time for chemical reactions, θ is the mean time of macroscopic parameters variation. In this case for the description of the non-equilibrium flow it is necessary to consider the equations of the state-to-state vibrational and chemical kinetics coupled to the

gas dynamic equations. It is the most detailed description of the non-equilibrium flow. Transport properties in the flow depend not only on gas temperature and mixture composition but also on all vibrational level populations of different species [20].

More simple models of the flow are based on quasi-stationary multi-temperature or one-temperature vibrational distributions. In the vibrationally excited gas at moderate temperatures, the near-resonant vibrational energy exchanges between molecules of the same chemical species occur much more frequently compared to the non-resonant transitions between different molecules as well as transfers of vibrational energy to the translational and rotational ones and chemical reactions:

$$\tau_{el} \sim \tau_{rot} < \tau_{VV_1} \ll \tau_{VV_2} < \tau_{TRV} < \tau_{react} \sim \theta \qquad (2)$$

Here τ_{VV_1}, τ_{VV_2}, τ_{TRV} are, respectively, the mean times for the VV_1 vibrational energy exchange between molecules of the same species, VV_2 vibrational transitions between molecules of different species and TRV transitions of the vibrational energy into other modes.

Under this condition quasi-stationary (multi-temperature) distributions over the vibrational levels establish due to rapid energy exchanges, and equations for vibrational level populations are reduced to the equations for vibrational temperatures for different chemical species. Heat and mass transfer are specified by the gas temperature, molar fractions of species and vibrational temperatures of molecular components [21].

For tempered reaction regime, with the chemical reaction rate considerably lower than that for the internal energy relaxation, the following characteristic time relation takes place:

$$\tau_{el} < \tau_{int} \ll \tau_{react} \sim \theta \qquad (3)$$

τ_{int} is the mean time for the internal energy relaxation. Under this condition, the non-equilibrium chemical kinetics can be described on the basis of the maintaining thermal equilibrium one-temperature Boltzmann distributions over internal energies of molecular species while transport properties are defined by the gas temperature and molar fractions of mixture components [9, 10]. The influence of electronic excitation of atoms and molecules on the transport properties under the last condition is also considered in Ref. [22].

4.1   State-to-state model

In the state-to-state approach [20], the closed set of equations for the macroscopic parameters includes the conservation equations of momentum and total energy coupled to the equations of detailed state-to-state vibrational and chemical kinetics:

$$\frac{dn_{ci}}{dt} + n_{ci}\nabla \cdot \mathbf{v} + \nabla \cdot (n_{ci}\mathbf{V}_{ci}) = R_{ci}, \quad c = 1, \cdots, L, \; i = 0,1, \cdots, L_c \;, \qquad (4)$$

$$\rho \frac{d\mathbf{v}}{dt} + \nabla \cdot \boldsymbol{P} = 0 \;, \qquad (5)$$

$$\rho \frac{dU}{dt} + \nabla \cdot \mathbf{q} + \boldsymbol{P} : \nabla \mathbf{v} = 0. \qquad (6)$$

Here n_{ci} is the population of vibrational level i of species c, $\mathbf{v}$ is the gas velocity, U is is the total energy per unit mass including translational, rotational, vibrational, and formation specific energy, $\boldsymbol{P}$ is the pressure tensor, $\mathbf{q}$ is the total energy flux, $\mathbf{V}_{ci}$ are diffusion velocities of molecules at different vibrational states, L is the number of species in a mixture, L_c is the number of vibrational levels in a molecular species c. The source terms R_{ci} in the equations (4) characterize the variation of the vibrational level populations and atomic number densities caused by different vibrational energy exchanges and chemical

reactions.

The feature of the state-to-state approach is that the vibrational level populations are included to the set of main macroscopic parameters, and the equations for their calculation are coupled to the equations of gas dynamics. Particles of various chemical species in different vibrational states represent the mixture components, and the corresponding equations contain the diffusion velocities $\mathbf{V}_{ci}$ of molecules at different vibrational states.

The set of state-to-state governing equations (4)-(6) in the inviscid (Euler) flow approximation, when $\mathbf{q}=\mathbf{V}_{ci}=0$, $\boldsymbol{P}=p\boldsymbol{I}$, was solved by many authors for shock heated (Adamovich et al; Kustova, Nagnibeda et al) and expanding flows (Capitelli, Colonna et al; Shizgal, Lordet; Park, Alexandrova et al). Appropriate references can be found in [10].

In the viscous flow approximation, the stress tensor is described by the expression [10, 20]:

$$\boldsymbol{P} = (p - p_{rel})\boldsymbol{I} - 2\eta\boldsymbol{S} - \zeta\nabla\cdot\mathbf{v}\boldsymbol{I} . \tag{7}$$

Here, p_{rel} is the relaxation pressure, η and ζ are the coefficients of shear and bulk viscosity, p is the pressure, $\boldsymbol{I}$ and $\boldsymbol{S}$ are the unit and deformation rate tensors. The additional terms connected to the bulk viscosity and relaxation pressure appear in the diagonal terms of the stress tensor in this case due to rapid inelastic TR exchange between the translational and rotational energies. The existence of the relaxation pressure is caused also by slow processes of vibrational and chemical relaxation. If all slow relaxation processes in a system disappear, then $p_{rel} = 0$.

The diffusion velocity $\mathbf{V}_{ci}$ of molecular components c at the vibrational level i is specified in the state-to-state approach by the expression [10, 20]:

$$\mathbf{V}_{ci} = -\sum_{dk} D_{cidk}\mathbf{d}_{dk} - D_{T_{ci}}\nabla\ln T, \tag{8}$$

where D_{cidk} and $D_{T_{ci}}$ are the multi-component diffusion and thermal diffusion coefficients for each chemical and vibrational species, T is the gas temperature, $\mathbf{d}_{ci}$ are the diffusive driving forces for each vibrational level (ρ_{ci} is the corresponding mass density)

$$\mathbf{d}_{ci} = \nabla\left(\frac{n_{ci}}{n}\right) + \left(\frac{n_{ci}}{n} - \frac{\rho_{ci}}{\rho}\right)\nabla\ln p.$$

The total energy flux in the first-order approximation has the form:

$$\mathbf{q} = -\lambda\nabla T - p\sum_{ci}D_{T_{ci}}\mathbf{d}_{ci} + \sum_{ci}\left(\frac{5}{2}kT + \langle\varepsilon^{ci}\rangle_{rot} + \varepsilon_i^c + \varepsilon_c\right)\mathbf{V}_{ci} , \tag{9}$$

where $\lambda = \lambda_{tr} + \lambda_{rot}$ is the thermal conductivity coefficient, $\langle\varepsilon^{ci}\rangle_{rot}$ is the mean rotational energy, k is the Boltzmann constant, ε_i^c is the vibrational energy of a molecule of species c at the i-th vibrational level, ε_c is the energy of formation of the particle of species c. The coefficients λ_{tr} and λ_{rot} are responsible for the energy transfer associated with the most probable processes which, in the present case, are the elastic collisions and inelastic TR- and RR rotational energy exchanges. In the state-to-state approach, the transport of the vibrational energy is described by the diffusion of vibrationally excited molecules rather than the thermal conductivity. In particular, the diffusion of the vibrational energy is simulated by introducing the independent diffusion coefficients for each vibrational state. It should be noted that all transport coefficients are specified by the cross sections of rapid processes except the relaxation pressure depending also on the cross sections of slow processes of vibrational relaxation and chemical reactions.

The set of equations (4)-(6) in the viscous approximation was solved only in such simple formulations as

boundary layer approximation in the vicinity of the stagnation point (Candler; Capitelli, Armenise et al; Josyula, see references in [10]).

Practical implementation of the state-to-state kinetic model is rather difficult mainly due to its computational cost. Indeed, the solution of the fluid dynamics equations coupled to the equations of the state-to-state vibrational and chemical kinetics in multi-component mixtures requires numerical simulation of a great number of equations for the vibrational level populations of all molecular species. Moreover, in the viscous gas approximation, numerical simulations require the calculation of a large number of transport coefficients, particularly, diffusion coefficients in each space cell and at each time step, which significantly complicates the study of specific flows. Therefore simpler models based on quasi-stationary vibrational distributions are rather attractive for practical applications.

4.2   Multi-temperature model

In quasi-stationary approaches, the vibrational level populations are expressed in terms of a few macroscopic parameters; consequently, non-equilibrium kinetics can be described by a considerably reduced set of governing equations. Commonly used models are based on the Boltzmann distribution with the vibrational temperature different from the gas temperature. However, such a distribution is valid solely for the harmonic oscillator model, which describes adequately only the low vibrational states. The more accurate quasi-stationary model is based on the Treanor two-temperature vibrational distribution for anharmonic oscillators [21, 10].

A closed system of reacting multi-component mixture dynamics consists of the equations of the multi-temperature chemical kinetics for the species number densities n_c, conservation equations for the momentum and the total energy, and additional energy relaxation equations for molecular species:

$$\frac{dn_c}{dt} + n_c \nabla \cdot \mathbf{v} + \nabla \cdot (n_c \mathbf{V}_c) = R_c^{react}, \quad c = 1, \cdots, L, \tag{10}$$

$$\rho \frac{d\mathbf{v}}{dt} + \nabla \cdot \boldsymbol{P} = 0 , \tag{11}$$

$$\rho \frac{dU}{dt} + \nabla \cdot \mathbf{q} + \boldsymbol{P} : \nabla \mathbf{v} = 0 , \tag{12}$$

$$\rho_c \frac{dW_c}{dt} + \nabla \cdot \mathbf{q}_{w,c} = R_c^w - m_c W_c R_c^{react} + W_c \nabla \cdot (\rho_c \mathbf{V}_c), \quad c = 1, \cdots, L_m . \tag{13}$$

Here $\mathbf{V}_c$ are diffusion velocities of different chemical species, W_c is a specific number of vibrational quanta in molecules of c species, $\mathbf{q}_{w,c}$ is the flux of vibrational quanta of c molecular species. R_c^{react} is the production term due to chemical reactions, R_c^w describes the production of vibrational energy due to VT processes and vibrational-chemical coupling.

In the first-order approximation, the stress tensor is expressed by Eq.(7). The diffusion velocity takes the form

$$\mathbf{V}_c = - \sum_d D_{cd} \mathbf{d}_d - D_{T_c} \nabla \ln T , \tag{14}$$

D_{cd} and D_{T_c} are the diffusion and thermal diffusion coefficients.

The total energy flux and the fluxes of vibrational quanta depend on the gradients of the gas temperature T, the temperatures of the first vibrational level T_1^c, and the molar fractions of chemical species n_c/n:

$$\mathbf{q} = -(\lambda + \sum_c \lambda_{vt}^c)\nabla T - \sum_c (\lambda_{tv}^c + \lambda_{vv}^c)\nabla T_1^c - p \sum_c D_{T_c} \mathbf{d}_c + \sum_c \rho_c h_c \mathbf{V}_c \, , \qquad (15)$$

$$\varepsilon_1^c \, \mathbf{q}_{w,c} = -\lambda_{vt}^c \nabla T - \lambda_{vv}^c \nabla T_1^c . \qquad (16)$$

In Eqs.(15), (16), λ, λ_{vt}^c, λ_{tv}^c, λ_{vv}^c are various thermal conductivity coefficients, h_c is the specific enthalpy of c particles. The coefficient λ describes the transport of the translational, rotational energy and a small part of the vibrational energy, which is transferred to the translational mode as a result of the non-resonant VV_1 transitions between molecules simulated by anharmonic oscillators and is presented as a sum of three corresponding terms: $\lambda = \lambda_{tr} + \lambda_{rot} + \lambda_{anh}$. The coefficients λ_{vv}^c are associated with the transport of vibrational quanta in each molecular species and thus describe the transport of the main part of vibrational energy $\varepsilon_1^c W_c$. The cross coefficients λ_{vt}^c, λ_{tv}^c are specified by both the transport of vibrational quanta and the vibrational energy loss (or gain) as a result of non-resonant VV_1 transitions. For low values of the ratio T_1^c/T, the coefficients λ_{anh}, λ_{vt}^c, and λ_{tv}^c are much smaller compared to λ_{vv}^c, and for the harmonic oscillator model $\lambda_{vt}^c = \lambda_{tv}^c = \lambda_{anh} = 0$ since VV_1 transitions appear to be strictly resonant.

The number of independent diffusion coefficients in the multi-temperature model is considerably smaller than that in the approach accounting for the detailed vibrational kinetics. Therefore the use of the quasi-stationary vibrational distributions noticeably facilitates the heat fluxes calculation in a multi-component reacting gas mixture. The proposed kinetic theory was applied in Ref. [23] for the simulation of gas-dynamic parameters, transport coefficients and heat fluxes in non-equilibrium reacting air flows behind strong shock waves.

4.3   One-temperature model

In the one-temperature approach based on the thermal equilibrium Boltzmann vibrational distributions, the closed set of governing equations includes equations for n_c, $\mathbf{v}$, T which have the form (10), (11), (12). However, one should keep in mind that transport and relaxation terms in these equations differ from those obtained in the multi-temperature approach because they are defined by different collision processes: in the one-temperature approximation rapid processes include along with elastic collisions all internal energy transitions while slow processes are specified by only chemical reactions. The total heat flux is described by the expression:

$$\mathbf{q} = -\lambda \nabla T - p \sum_c D_{T_c} \mathbf{d}_c + \sum_c \rho_c h_c \mathbf{V}_c \, , \qquad (17)$$

where $\lambda = \lambda_{tr} + \lambda_{rot} + \lambda_{vibr}$, λ_{vibr} is the vibrational thermal conductivity coefficient. In this approach the bulk viscosity and relaxation pressure in the stress tensor are specified by both rotational and vibrational degrees of freedom $\zeta = \zeta_{rot} + \zeta_{vibr}$, $p_{rel} = p_{rel}^{rot} + p_{rel}^{vibr}$.

4.4   Comparison of different models

The heat flux calculated in the frame of the state-to-state, two-temperature and one-temperature models behind the plane shock wave [10] is presented in Fig. 9. N_2/N mixture was studied under the following conditions in the free stream: $T_0 = 293$ K, $p_0 = 100$ Pa, $M_0 = 15$. The one-temperature and two-temperature approaches substantially underestimate the absolute values for the heat flux in the very beginning of the relaxation zone, where the process of vibrational excitation is essential. The more rigorous state-to-state approach should be applied close to the shock front ($x < 0.3$ cm, or about twenty mean free path lengths in the unperturbed flow), in the domain of simultaneous vibrational relaxation and chemical reactions.

Similar analysis was performed for the nozzle expansion. In Fig. 10, the heat flux calculated using the state-to-state, two-temperature models for harmonic and anharmonic oscillators, and one-temperature model in a conic nozzle is given. The heat flux decreases with x, since the gradients of the macroscopic parameters also decrease with the distance from the throat. While the one-temperature model yields

underestimated heat flux, the two-temperature quasi-stationary models provide a satisfactory accuracy for **q**. The deviation of the heat flux found in the non-equilibrium quasi-stationary approaches from that obtained within the most rigorous state-to-state model is 4 and 10% for anharmonic and harmonic oscillators, respectively.
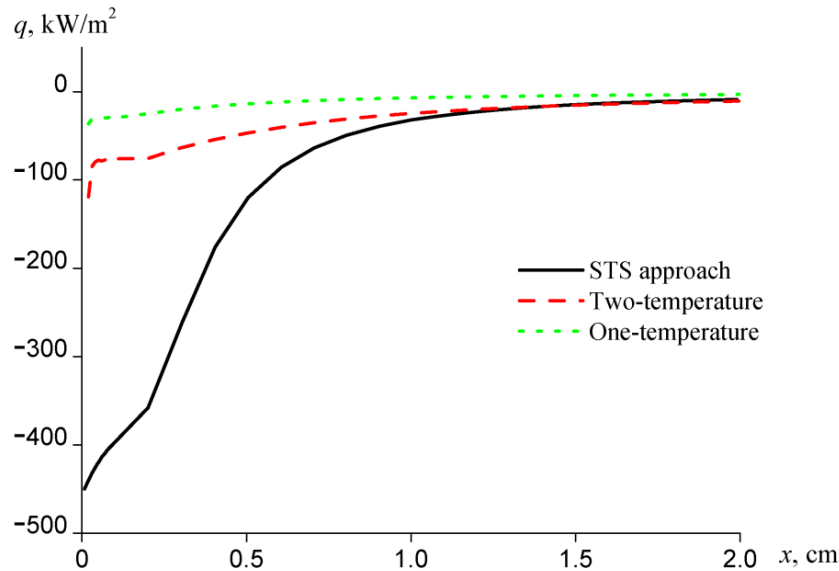

Figure 9: The heat flux q as a function of *x* behind a shock wave. *T₀* = 293 K, *p₀* = 100 Pa, M₀ = 15. Different curves represent the state-to-state, two-temperature, and one-temperature approaches.
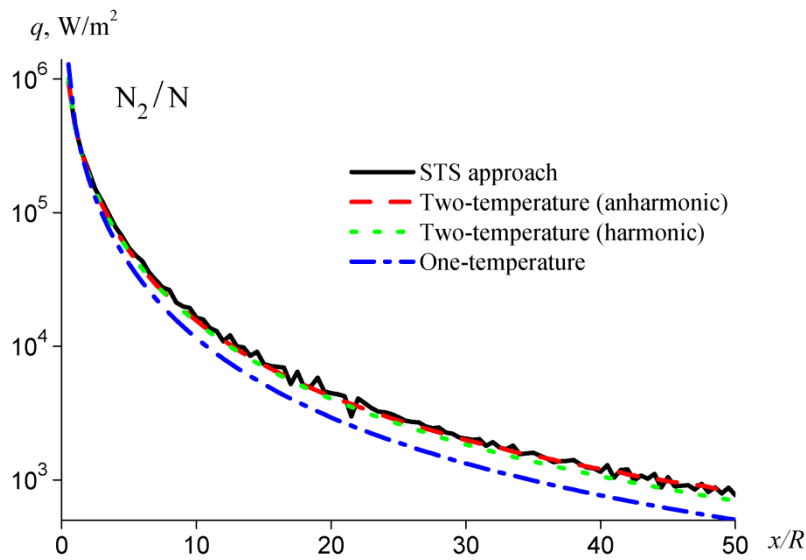

Figure 10: The heat flux q as a function of *x/R* in a nozzle. *R* is the throat radius, *T₀* = 7000 K, *p₀* = 100 atm. Different curves represent the state-to-state, two-temperature for harmonic and anharmonic oscillators, and one-temperature approaches.

4.5 Contribution of various processes to the state-to-state heat flux

Let us consider the contribution of different processes to diffusion and heat transfer. For the sake of simplicity, we will consider a binary mixture A_2/A. In this case, for the diffusion velocities of molecules at

the i-th level $\mathbf{V}_i$ and atoms $\mathbf{V}_a$ we have

$$\mathbf{V}_i = \mathbf{V}_i^{TD} + \mathbf{V}_i^{MD} + \mathbf{V}_i^{DVE} \tag{18}$$

$$\mathbf{V}_a = \mathbf{V}_a^{TD} + \mathbf{V}_a^{MD} \tag{19}$$

Here, $\mathbf{V}_i^{MD}$, $\mathbf{V}_a^{MD}$, $\mathbf{V}_i^{TD}$, $\mathbf{V}_a^{TD}$, and $\mathbf{V}_i^{DVE}$ are, respectively, the contributions of the mass diffusion, thermal diffusion, and diffusion of vibrational energy

$$\mathbf{V}_i^{MD} = -D_{mm}\mathbf{d}_m - D_{ma}\mathbf{d}_a$$

$$\mathbf{V}_i^{TD} = -D_{Tm}\nabla \ln T$$

$$\mathbf{V}_i^{DVE} = -\widetilde{D}\nabla \ln \frac{n_i}{n_m}$$

$$\mathbf{V}_a^{MD} = -D_{ma}\mathbf{d}_m - D_{aa}\mathbf{d}_a$$

$$\mathbf{V}_a^{TD} = -D_{Ta}\nabla \ln T$$

Subscripts "m" and "a" correspond to molecules A_2 and atoms A, respectively, $\widetilde{D}$ is the fictitious diffusion coefficient. It is obvious that $\mathbf{V}_i^{TD}$, $\mathbf{V}_i^{MD}$ do not depend on the vibrational state i of a molecule and are specified only by its chemical species. These terms formally coincide with the corresponding terms in the relations for the diffusion velocity in the multi-temperature and one-temperature approaches. The difference is determined by the fact that the transport coefficients in these expressions depend on the cross sections of various processes. If we assume, that the diffusion and thermal diffusion coefficients are specified by the cross sections of only elastic collisions, we find

$$\mathbf{V}_i = \mathbf{V}_m^{QS} + \mathbf{V}_i^{DVE}$$

where $\mathbf{V}_m^{QS}$ is the diffusion velocity of molecules in the quasi-stationary approach, the second term appears only in the state-to-state approach.

The contribution of several dissipative processes to the heat flux can be also distinguished:

$$\mathbf{q} = \mathbf{q}^{HC} + \mathbf{q}^{MD} + \mathbf{q}^{TD} + \mathbf{q}^{DVE} \tag{20}$$

where $\mathbf{q}^{HC}$, $\mathbf{q}^{MD}$, $\mathbf{q}^{TD}$, and $\mathbf{q}^{DVE}$ are, respectively, energy fluxes associated with the heat conductivity of translational and rotational degrees of freedom, mass diffusion, thermal diffusion, and the transfer of vibrational energy

$$\mathbf{q}^{HC} = -\lambda\nabla T$$

$$\mathbf{q}^{MD} = \rho_m h_m \mathbf{V}_m^{MD} + \rho_a h_a \mathbf{V}_a^{MD}$$

$$\mathbf{q}^{TD} = -p(D_{Tm}\mathbf{d}_m + D_{Ta}\mathbf{d}_a) + \rho_m h_m \mathbf{V}_m^{TD} + \rho_a h_a \mathbf{V}_a^{TD}$$

$$\mathbf{q}^{DVE} = \sum_i \left(\frac{5}{2}kT + \langle\varepsilon_j^i\rangle_{rot} + \varepsilon_i\right) n_i \mathbf{V}_i^{DVE}$$

We can notice that only $\mathbf{q}^{DVE}$ depends explicitly on the non-equilibrium state-to-state vibrational distributions, while the remaining components in Eq. (20) are similar to the corresponding terms in the

expressions for the heat flux in the quasi-stationary approaches.

The expressions given above permit to perform a simple limit transition from the equation for the heat flux in the state-to-state approximation to the corresponding relations in the quasi-stationary approaches. Thus, if in a binary mixture of molecules and atoms the quasi-stationary two-temperature or one-temperature vibrational distribution is established in the zero-order approximation, then, assuming the independence of transport coefficients of the cross sections for inelastic collisions, we can obtain the expression for the heat flux directly substituting the quasi-stationary distribution into the formula for $\mathbf{q}^{DVE}$ in the state-to-state approach. A similar limit transition can also be performed for a multi-component gas mixture.
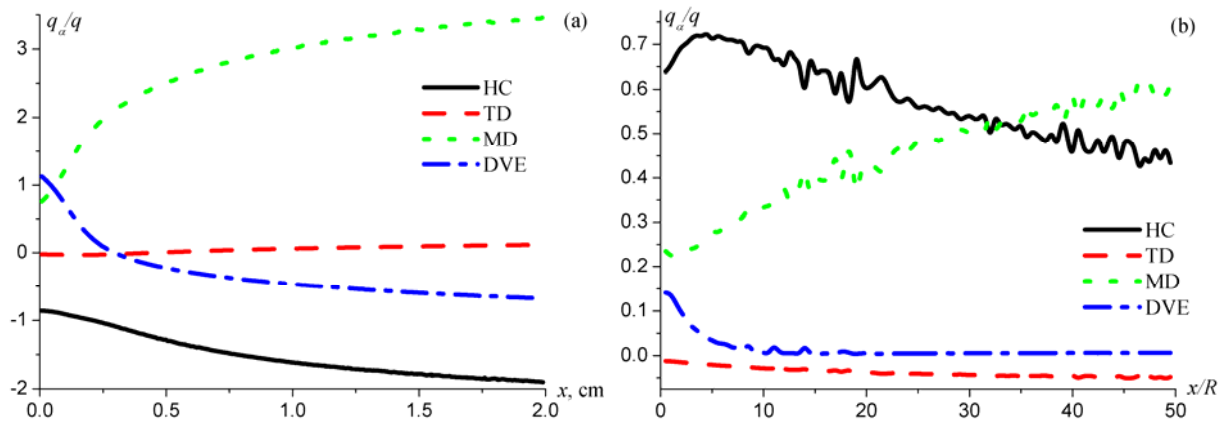

Figure 11: Ratio of the heat flux due to various processes (α = HC, TD, MD, DVE) to the total heat flux q (a) behind the shock wave as a function of *x*, and (b) in a conic nozzle as a function of *x/R*.

Fig. 11 shows the contribution of different transport processes in the mixture (N$_2$,N) to the heat flux variation behind a shock wave and in a nozzle flow along its axis. The flow conditions are the same as in Figs. 9, 10. One can see that the contribution of thermal diffusion to the heat flux is small in both flows while mass diffusion of atoms is important in the whole flow region. Diffusion of vibrationally excited molecules plays more important role behind a shock than in a nozzle. Close to the shock front, heat conduction and mass diffusion compensate each other, and the main role in the heat transfer belongs to the diffusion of vibrational states. In an expanding flow, $\mathbf{q}^{DVE}$ is not negligible only close to the throat (but does not exceed 15%).

4.6   On the comparison of experimental data and theoretical calculations

An important problem in rarefied aerodynamics is the validation of theoretical results against experimental data. In real gas flows, collision cross sections decrease with the relative particle velocity. Let us assume, for instance, that we use the hard sphere model for theoretical calculations. Then, while comparing theoretical and experimental results, we can obtain reliable data only if we assume the cross section for hard spheres to be equal to the real cross section for collisions between incident and reflected particles, and if the transition to the free stream parameters is carried out accordingly to the real law of molecular interaction. Moreover, we should keep in mind that for the same gas, the transition to the free stream parameters in wind tunnel experiments (WTE) and in natural full-scale experiments (FSE) can be different. In wind tunnels at high Mach numbers, the free stream temperature T_∞ is commonly lower than that in natural flows for the same values of M. Therefore, the relative molecular velocity in the free stream is lower in WTE than in FSE, and the rate of variation of the cross section is different. Consequently, it can happen that while in the wind tunnel the molecules behave as the Maxwell ones, in the natural flow they can be described by hard spheres with constant cross sections. Sometimes the calculations based on the hard sphere model agree with the flight experiments for given M and Kn numbers, but, at the same

time, they correspond to the WTE with the different Knudsen number.

Let us assume roughly that in wind tunnels we have Maxwell molecules with the cross section inversely proportional to the relative velocity. Denote Kn_{HS} the Knudsen number for hard spheres, and $Kn_{\infty,WT}$ the free stream Knudsen number in WTE. Then theoretical results can be consistent with experimental data only if we choose [5]

$$Kn_{HS} = Kn_{\infty,WT} \ M$$

On the contrary, calculations performed for Maxwell molecules with Kn_M are consistent with WTE for the same M and Kn. However, to compare them with FSE, we should perform calculations for

$$Kn_M = \ Kn_{\infty,FS} \ /M$$

Also we should note that while passing from WTE to FSE, we cannot compare the data obtained for the same M and Kn in the free stream. Experiments conducted at different free stream temperatures can be considered as those carried out for different gases since the viscosity varies differently with the temperature.

The above reasoning is rather approximate and can be applied only for rough estimates. Strictly speaking, in order to provide similarity in flows around geometrically similar bodies, we should require identity for the following parameters: Kn, M, T_w/T_∞, σ, α. The similarity according to the Reynolds number Re is the consequence of the similarity with respect to M and Kn.

5.0   CONCLUSIONS

The main peculiarities of rarefied flows in different regimes are discussed. Various theoretical approaches are suitable for different regimes: the free-molecular flows are satisfactory described by the kinetic theory; in transition regimes, DSMC is the best choice; and for non-equilibrium slip flows, asymptotic methods such as modifications of the Chapman-Enskog method provide a good description. A brief overview of experimental methods for rarefied aerodynamics is given, and the facilities VU-1 and TB-3 of Saint Petersburg State University are described in details. Comparison of various theoretical models shows the advantages of state-to-state modeling in non-equilibrium reacting flows.

6.0   REFERENCES

[1]   Chapman, S., Cowling, T.: The Mathematical Theory of Non-Uniform Gases, 3rd edn., Cambridge University Press, Cambridge (1970)

[2]   Grad, H.: On the kinetic theory of rarefied gases. Comm. Pure Appl. Math. 2, 331 (1949)

[3]   Rarefied Gas Dynamics, ed. by. F.M. Devienne, Proceedings of the 1st Int. Symp. on Rarefied Gas Dynamics, Pergamon press, London, Oxford, New-York, Paris (1960)

[4]   Aerodynamics of Rarefied Gases, ed. by S. Vallander, S., vol. I. Leningrad University Press, Leningrad (1963) (in Russian)

[5]   Kogan, M.: Rarefied Gas Dynamics. Nauka, Moscow (1967); English transl. Plenum Press, New York (1969)

[6]   Cercignani, C.: Theory and Application of the Boltzmann Equation, Scottish Academic Press,

Edinburgh and London (1975)

[7]   Vallander, S., Nagnibeda, E., Rydalevskaya, M.: Some Questions of the Kinetic Theory of the Chemical Reacting Gas Mixture. Leningrad University Press, Leningrad (1977); English Transl. US Air Force FASTC–ID (RS) TO–0608–93

[8]   Brun, R.: Transport et relaxation dans les écoulements gazeux. Masson, Paris, New York, Barselone, Milan, Mexico, Saõ Paulo (1986)

[9]   Giovangigli, V.: Multicomponent Flow Modeling, Birkhauser, Boston, 1999.

[10]   Nagnibeda, E., Kustova, E.: Nonequilibrium Reacting Gas Flows. Kinetic Theory of Transport and Relaxation Processes, Springer Verlag, Berlin, Heidelberg, 2009.

[11]   Brun, R.: Introduction to Reactive Gas Dynamics, Oxford University Press, 2009.

[12]   Bird, G.: Molecular Gas Dynamics, Clarendon, Oxford (1976)

[13]   Bird, G.: Molecular Gas Dynamics and the Direct Simulation of Gas Flows, Claredon, Oxford (1994)

[14]   Mashek I.Ch., Anisimov Yu. I., Ivanov V.I., Kolesnichenko Yu. F., Ryvkin M.I., Gorynya A.A. Gas Dynamic Effect of Microwave Discharge on Supersonic Cone-shaped Bodies // Paper AIAA 2004-671. 42nd AIAA Airspace Science Meeting and Exhibit, 5-8 January 2004, Reno, NV, USA.

[15]   Mashek I.Ch., Anisimov Yu. I., Kolesnichenko Yu. F., Azarova O.A., Ivanov V.I. Method of Vortex Flow Intensification Under MW Filament Interaction with Shock Layer on Supersonic Body // Paper AIAA 2006-0404. 44-th AIAA Aerospace Science Meeting and Exhibit 9-12 January 2006, Reno, NV, USA.

[16]   Eucken, E.: Physik. Zeitschr., 14, 324–332 (1913)

[17]   Ferziger, J., Kaper, H.: Mathematical Theory of Transport Processes in Gases, North-Holland, Amsterdam (1972)

[18]   Stupochenko, Y., Losev, S., Osipov, A.: Relaxation in Shock Waves, Nauka, Moscow (1965); Engl.transl. Springer, Heidelberg (1967)

[19]   Chernyi, G., Losev, S. (eds.), Physical-Chemical Processes in Gas Dynamics, vol. 1,2, Moscow University Press, Moscow (1995)

[20]   Kustova, E., Nagnibeda, E.: Chem. Phys, 233, 57–75 (1998)

[21]   Chikhaoui, A., Dudon, J., Kustova, E., Nagnibeda, E.: Physica A, 247(1-4), 526–552 (1997)

[22]   Kustova, E., Puzyreva, L.: Phys. Rev. E, 80 (No. 4), 046407 (2009)

[23]   Chikhaoui, A., Dudon, J., Genieys, S., Kustova, E., Nagnibeda, E.: Phys. Fluids, 12(1), 220–232 (2000)